J|A|C|S
ARTICLES
Published on Web 06/17/2006

Preparation and Structure of $CeSc_2N@C_{80}$: An Icosahedral Carbon Cage Enclosing an Acentric $CeSc_2N$ Unit with Buried f Electron Spin

Xuelei Wang,[†] Tianming Zuo,[†] Marilyn M. Olmstead,[‡] James C. Duchamp,[§] Thomas E. Glass,[†] Frank Cromer,[†] Alan L. Balch,*[,‡] and Harry C. Dorn*[,†]

Contribution from the Department of Chemistry, Virginia Polytechnic Institute and State University, Blacksburg, Virginia 24061, Department of Chemistry, University of California at Davis, Davis, California 95616, and Department of Chemistry, Emory & Henry College, Emory, Virginia 24327

Received March 1, 2006; E-mail: albalch@ucdavis.edu; hdorn@vt.edu

Abstract: Herein, we report the preparation, purification, and characterization of a mixed trimetallic nitride endohedral metallofullerene, $CeSc_2N@C_{80}$. Single-crystal X-ray diffraction shows that $CeSc_2N@C_{80}$ consists of a four-atom asymmetric top ($CeSc_2N$) inside a C_{80} (I_h) carbon cage. Unlike the situation in most endohedrals of the $M_3N@C_{2n}$ type, the nitride ion is not located at the center of the carbon cage but is offset by 0.36 Å in order to accommodate the large Ce^{III} ion. The cage carbon atoms near the endohedral Ce and Sc atoms exhibit significantly larger pyramidal angles than the other carbon atoms on the C_{80} cage. Surprisingly, at ambient temperature, the ^{13}C NMR spectrum exhibits isotropic motional averaging yielding only two signals (3 to 1 intensity ratio) for the icosahedral C_{80} cage carbons. At the same temperature, the ^{45}Sc NMR exhibits a relatively narrow, symmetric signal (2700 Hz) with a small temperature-dependent Curie shift. A rotation energy barrier ($E_a = 79$ meV) was derived from the ^{45}Sc NMR line-width analysis. Finally, the XPS spectrum for $CeSc_2N@C_{80}$ confirms a +3 oxidation state for cerium, Ce^{3+}-($4f^15d^0$).This oxidation state and the Curie shift are consistent with a weakly paramagnetic system with a single buried f electron spin.

Introduction

Since the beginning of fullerene chemistry, metal-containing endohedral fullerenes have attracted particular interest since the encapsulated metal atoms can impart unusual physical and chemical properties.[1−6] Also, the metal can readily donate charge to the cage which in certain cases stabilizes reactive empty cage fullerenes, such as the IPR-obeying C_{74}[7] (IPR = isolated pentagon rule) and the non-IPR obeying C_{66}[8] and C_{68} cages.[9] However, progress in exploring the structures and properties of endohedal metallofullerenes (EMFs) has been hampered by their low production yields and by purification difficulties. Nevertheless, in the past two decades, scandium, cerium, praseodymium, terbium, gadolinium, neodymium, lanthanum, erbium, holmium, dysprosium, lutetium, thulium, samarium, europium, and ytterbium have been encapsulated to yield a mono- or dimetallofullerene species via the Krätschmer−Huffman electric-arc process.[7,10−18] In 1996, the cerium mono-metallofullerene and di-metallofullerene, $Ce@C_{82}$ and $Ce_2@C_{80}$, were synthesized by Yang and co-workers.[16] The UV−vis−NIR absorption spectra and XPS patterns suggested that cerium in both $Ce@C_{82}$ and $Ce_2@C_{80}$ should be in the Ce^{3+} oxidation state, although earlier *ab initio* calculation suggested that the electronic structure of $Ce@C_{82}$ should be formally described as $Ce^{2+}@C_{82}{}^{2-}$.[19] Recently, the magnetic properties of $Ce@C_{82}$

[†] Virginia Polytechnic Institute and State University.
[‡] University of California at Davis.
[§] Emory & Henry College.

(1) Shinohara, H. *Rep. Prog. Phys.* **2000**, *63*, 843−892.
(2) Akasaka, T.; Nagase, S. *Endofullerenes: A New Family of Carbon Clusters*; Kluwer Academic Publishers: Dordrecht, 2002.
(3) Dunsch, L.; Krause, M.; Noack, J.; Georgi, P. *J. Phys. Chem. Solids* **2004**, *65*, 309−315.
(4) Wilson, L. J.; Cagle, D. W.; Thrash, T. P.; Kennel, S. J.; Mirzadeh, S.; Alford, J. M.; Ehrhardt, G. J. *Coord. Chem. Rev.* **1999**, *190−192*, 199−207.
(5) Kato, H.; Kanazawa, Y.; Okumura, M.; Taninaka, A.; Yokawa, T.; Shinohara, H. *J. Am. Chem. Soc.* **2003**, *125*, 4391−4397.
(6) Sun, D.; Liu, Z.; Guo, X.; Xu, W.; Liu, S. *Fullerene Sci. Technol.* **1997**, *5*, 137−143.
(7) Kuran, P.; Krause, M.; Bartl, A.; Dunsch, L. *Chem. Phys. Lett.* **1998**, *292*, 580−586.
(8) Wang, C. R.; Kai, T.; Tomiyama, T.; Yoshida, T.; Kobayashi, Y.; Nishibori, E.; Takata, M.; Sakata, M.; Shinohara, H. *Nature* **2000**, *408*, 426−427.
(9) Stevenson, S.; Fowler, P. W.; Heine, T.; Duchamp, J. C.; Rice, G.; Glass, T.; Harich, K.; Hajdu, E.; Bible, R.; Dorn, H. C. *Nature* **2000**, *408*, 427−428.
(10) Lebedkin, S.; Renker, B.; Heid, R.; Schober, H.; Rietschel, H. *Appl. Phys. A* **1998**, *66*, 273−280.
(11) Ding, J. Q.; Yang, S. H. *J. Am. Chem. Soc.* **1996**, *118*, 11254−11257.
(12) Gu, G.; Huang, H. J.; Yang, S. H.; Yu, P.; Fu, J. S.; Wong, G. K.; Wan, X. G.; Dong, J. M.; Du, Y. W. *Chem. Phys. Lett.* **1998**, *289*, 167−173.
(13) Hino, S.; Umishita, K.; Iwasaki, K.; Miyazaki, T.; Miyamae, T.; Kikuchi, K.; Achiba, Y. *Chem. Phys. Lett.* **1997**, *281*, 115−122.
(14) Grannan, S. M.; Birmingham, J. T.; Richards, P. L.; Bethune, D. S.; De Vries, M. S.; Van Loosdrecht, P. H. M.; Dorn, H. C.; Burbank, P.; Bailey, J.; Stevenson, S. *Chem. Phys. Lett.* **1997**, *264*, 359−365.
(15) Ding, X. Y.; Alford, J. M.; Wright, J. C. *Chem. Phys. Lett.* **1997**, *269*, 72−78.
(16) (a) Ding, J. Q.; Weng, L. T.; Yang, S. H. *J. Phys. Chem.* **1996**, *100*, 11120−11121. (b) Ding, J. Q.; Yang, S. H. *Angew. Chem., Int. Ed. Engl.* **1996**, *35*, 2234−2235.
(17) Okazaki, T.; Lian, Y.; Gu, Z.; Suenaga, K.; Shinohara, H. *Chem. Phys. Lett.* **2000**, *320*, 435−440.

10.1021/ja061434i CCC: $33.50 **© 2006 American Chemical Society**

have been investigated by examining the magnetic field-induced changes in the magnetic susceptibility of $Ce@C_{82}$.[20] The magnetic anisotropy of cerium endohedral metallofullerenes is believed to be associated with the off-center geometry of the Ce^{3+} ion in the cage.[20]

In 1999, our laboratories reported the synthesis and characterization of novel trimetallic nitride template (TNT) endohedral metallofullerenes in high yields, by introducing nitrogen gas into the Krätschmer−Huffman generator.[21] Since this discovery, many new members of this interesting family, e.g., $A_3N@C_{80}$ (A = Er,[21] Gd,[22,23] Ho,[24] Tb,[25] Dy,[26] Tm,[27] Lu,[28] Y[29]) have been reported with the nitrogen atom located at the geometric center of the molecule. For example, the most common trimetallic nitride, $Sc_3N@C_{80}$, can be formally viewed as a positively charged planar tetra-atom cluster inside a negatively charged icosahedral (I_h) carbon cage, $[Sc_3N]^{+6}@[C_{80}]^{-6}$.[30c,31] Each scandium atom transfers one electron to the nitrogen atom and two electrons to the carbon cage which forms a stabilized closed-shell electronic structure $[C_{80}]^{-6}$.[30] In an earlier ^{13}C NMR study, the existence of a second isomer of $Sc_3N@C_{80}$ (D_{5h})[32] was established, and its structure was confirmed in a recent X-ray crystallographic study.[33] Also, other examples of D_{5h} isomers have been reported for $Dy_3N@C_{80}$,[26] $Tm_3N@C_{80}$,[27] and a third isomer of $Dy_3N@C_{80}$ has been reported.[34] Until now no X-ray crystallographic structures have been reported for these cases. In contrast to the homonuclear A_3N cluster, there is a paucity of mixed metal cluster cases (AB_2N) reported to date. A notable exception is $ErSc_2N@C_{80}$ which has been characterized by a single-crystal X-ray diffraction study.[35] Another series of mixed-metal species of TNT-EMFs, $Lu_{3-x}A_xN@C_{80}$ (x = 1, 2; A = Ho, Gd), were prepared in 2002,[28a] but these have not been isolated and characterized. With the exceptions noted above, most mixed-metal (AB_2N) based TNT-EMFs have not been isolated in pure form because of difficulties in the separation and purification process. We now report the first synthesis, structure, and characterization of $CeSc_2N@C_{80}$.

Experimental Section

Production of $CeSc_2N@C_{80}$. Graphite rods (0.25 in. diameter, 6 in. length) were core-drilled and subsequently packed with a mixture of graphite powder, Sc_2O_3, CeO_2, and Fe_xN (x = 2 to 4). The weight ratio of the components in the mixture is $C/Sc_2O_3/CeO_2/Fe_xN$ = 1.0:0.33:0.41:0.40. Fe_xN serves as a catalyst. These rods were then vaporized in a Krätschmer−Huffman generator under a dynamic flow of He and N_2 (flow rate ratio of N_2/He = 3:100) with a total pressure of ca. 300 Torr to obtain soot containing $CeSc_2N@C_{80}$. The resulting soot was then extracted with refluxing toluene for 20 h to obtain the initial endohedral extract. A portion of the negative ion desorption chemical ionization (NI-DCI) mass spectrum of the initial extract is shown in the Supporting Information.

Separation of $CeSc_2N@C_{80}$. The extract was applied to a glass column (28 cm × 22 mm, $h \times d$) packed with approximately 20 g of cyclopentadiene-functionized Merrifield resin in toluene. Toluene was flushed through by gravity feed (around 20 mL/h). The eluent was further separated using two-stage HPLC approaches. First, the pentabromobenzyloxypropyl silica, 5PBB, column (25 cm × 4.6 mm, Alltech Associates) was employed with toluene as the mobile phase. The peak of $CeSc_2N@C_{80}$ from this 5PBB column was collected and further separated with a 2-(1-pyrenyl)ethyl silica, 5PYE column (25 cm × 10 mm, Nacalai Tesque) using toluene as a mobile phase to obtain the purified $CeSc_2N@C_{80}$ sample. From five packed graphite rods, approximately 3.0 mg of purified $CeSc_2N@C_{80}$ was obtained. The NI-DCI mass spectrum and final HPLC trace are shown in Figure 1a.

UV−vis Spectrum of $CeSc_2N@C_{80}$. The spectra of $CeSc_2N@C_{80}$ and $Sc_3N@C_{80}$ (I_h) dissolved in toluene were recorded on a Cary 50 UV−vis spectrophotometer (Varian, USA).

XPS of $CeSc_2N@C_{80}$. A $CeSc_2N@C_{80}$ film was prepared on a gold foil. To clean the gold surface, a small piece of gold foil was dipped in acetone and dried in N_2 gas. Several drops of a concentrated solution of $CeSc_2N@C_{80}$ in carbon disulfide were transferred to the cleaned gold foil, and the evaporation of the solvent left a uniform film of $CeSc_2N@C_{80}$. The gold foil with the film on was heated at ca. 150 °C in a vacuum line for 20 min. The XPS spectrum was recorded on a Perkin-Elmer physical electronics model 5400 spectrometer.

NMR of $CeSc_2N@C_{80}$. The 125 MHz ^{13}C NMR spectrum of $CeSc_2N@C_{80}$ in CS_2/acetone-d_6 (v/v 9:1) was recorded on a JEOL 500 MHz instrument. Chromium(III) acetylacetonate (10 mg) was added as a relaxation agent. The 121.5 MHz ^{45}Sc NMR spectrum of $CeSc_2N@C_{80}$ in 1,2-dichlorobenzene at room temperature was recorded on a JEOL 500 MHz instrument, and the 97.2 MHz ^{45}Sc NMR spectra at various temperatures were recorded on a Unity 400 MHz instrument.

Crystal Growth for $CeSc_2N@C_{80}\cdot Ni^{II}(OEP)\cdot 2C_6H_6$. Crystals of $CeSc_2N@C_{80}\cdot Ni^{II}(OEP)\cdot 2C_6H_6$ were obtained by layering a solution of ca. 0.7 mg of $CeSc_2N@C_{80}$ in 0.5 mL of benzene over a solution of $Ni^{II}(OEP)$ in benzene. After the two solutions diffused together over a 14 day period, black crystals formed.

X-ray Crystallography and Data Collection. The crystals were removed from the glass tube in which they were grown together with a small amount of mother liquor and immediately coated with a hydrocarbon oil on the microscope slide. A suitable crystal was mounted on a glass fiber with silicone grease and placed on the goniometer head in the cold dinitrogen stream from a CRYO Industries low-temperature apparatus at 90(2) K. The diffractometer was Bruker SMART Apex with an Apex II CCD and utilized Mo Kα radiation. No decay was observed in 50 duplicate frames at the end of data collection. Crystal data are given below. The structure was solved by direct methods and refined using all data (based on F^2) with the software of SHELXTL 5.1. A semiempirical method utilizing equivalents was employed to correct for absorption.[36] Hydrogen atoms were added geometrically and refined with a riding model.

(18) Huang, H.; Yang, S. H. *J. Phys. Chem. Solids* **2000**, *61*, 1105−1110.
(19) Nagase, S.; Kobayashi, K. *Chem. Phys. Lett.* **1994**, *228*, 106−110.
(20) Inakuma, M.; Kato, H.; Taninaka, A.; Shinohara, H.; Enoki, T. *J. Phys. Chem. B* **2003**, *107*, 6965−6973.
(21) Stevenson, S. et al. *Nature* **1999**, *401*, 55−57.
(22) Stevenson, S.; Philips, J. P.; Reid, J. E.; Olmstead, M. M.; Rath, S. P.; Balch, A. L. *Chem. Commun.* **2004**, 2814−2815.
(23) Krause, M.; Dunsch, L. *Angew. Chem., Int. Ed.* **2005**, *44*, 1557−1560.
(24) Dunsch, L.; Georgi, P.; Krause, M.; Wang, C. R. *Synth. Met.* **2003**, *135*−*136*, 761−762.
(25) Feng, L.; Xu, J. X.; Shi, Z. J.; He, X. R.; Gu, Z. N. *Gaodeng Xuexiao Huaxue Xuebao* **2002**, *23*, 996−999.
(26) Yang, S. F.; Dunsch, L. *J. Phys. Chem. B* **2005**, *109*, 12320−12328.
(27) Krause, M.; Wong, J.; Dunsch, L. *Chem.−Eur. J.* **2005**, *11*, 706−711.
(28) (a) Iezzi, E.; Duchamp, J. C.; Fletcher, K. R.; Glass, T. E.; Dorn, H. C. *Nano Lett.* **2002**, *2*, 1187−1190. (b) Stevenson, S.; Lee, H. M.; Olmstead, M. M.; Kozikowski, C.; Stevenson, P.; Balch, A. L. *Chem.−Eur. J.* **2002**, *8*, 4528−4535.
(29) Dunsch, L.; Krause, M.; Noack, J.; Georgi, P. *J. Phys. Chem. Solid* **2004**, *65*, 309−315.
(30) (a) Kobayashi, K.; Nagase, S. *Chem. Phys. Lett.* **1996**, *262*, 227−232. (b) Kobayashi, K.; Nagase, S.; Akasaka, T. *Chem. Phys. Lett.* **1996**, *261*, 502−506. (c) Kobayashi, K.; Sano, Y.; Nagase, S. *J. Comput. Chem.* **2001**, *22*, 1353−1358.
(31) (a) Aihara, J. *J. Phys. Chem., Chem. Phys.* **2001**, *3*, 1427−1431. (b) Aihara, J. *Chem. Phys. Lett.* **2001**, *343*, 465−469. (c) Aihara, J. *J. Phys. Chem. A* **2002**, *106*, 11371−11374.
(32) Duchamp, J. C.; Demortier, A.; Fletcher, K. R.; Dorn, D.; Iezzi, E. B.; Glass, T. E.; Dorn, H. C. *Chem. Phys. Lett.* **2003**, *375*, 655−659.
(33) Cai, T.; Xu, L.; Anderson, M. R.; Ge, Z.; Zuo, T.; Wang, X.; Olmstead, M. M.; Balch, A. L.; Gibson, H. W.; Dorn, H. C. *J. Am. Chem. Soc.*, in press, **2006**.
(34) Yang, S.; Dunsch, L. *Chem.−Eur. J.* **2005**, *12*, 413−419.
(35) Olmstead, M. M.; de Bettencourt-Dias, A.; Duchamp, J. C.; Stevenson, S.; Dorn, H. C.; Balch, A. L. *J. Am. Chem. Soc.* **2000**, *122*, 12220−12226.
(36) SADABS 2.10, G. M. Sheldrick, based on a method of R. H. Blessing, *Acta Crystallogr., Sect. A* **1995**, *A51*, 33.

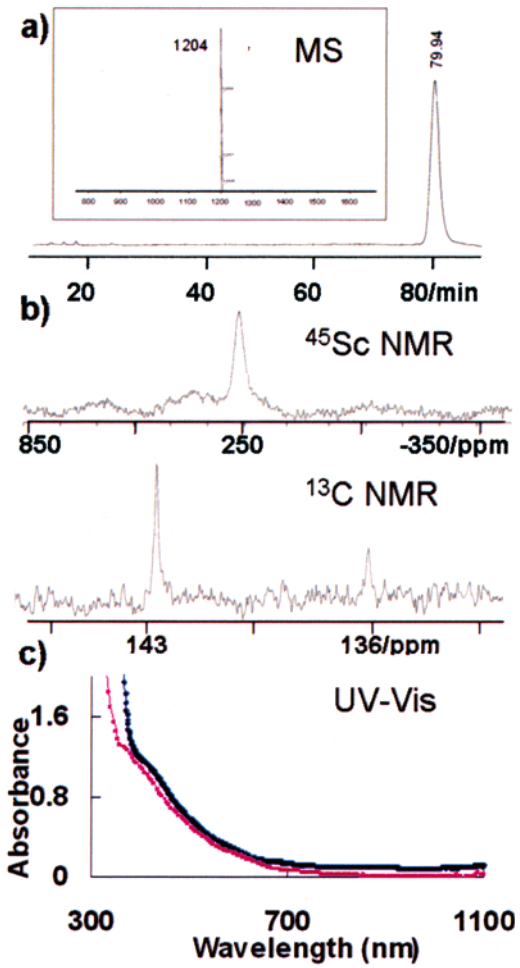

Figure 1. (a) The HPLC chromatogram for the purified sample of $CeSc_2N@C_{80}$ (5PYE column 10 mm × 250 mm, toluene as eluent at a flow rate of 1.0 mL/min, detector set at 390 nm) and the inset shows the NI-DCI mass spectrum of this sample. (b) 121.5 MHz ^{45}Sc NMR spectrum of $CeSc_2N@C_{80}$ in 1,2-dichlorobenzene (25 °C, 140,000 scans) and 125 MHz ^{13}C NMR spectrum of $CeSc_2N@C_{80}$ in CS_2/acetone-d_6 (v/v 9:1) (25 °C, $Cr(acac)_3$ added, 21,000 scans). (c) Comparison of the UV−vis absorption spectra of $CeSc_2N@C_{80}$ (deep blue) and $Sc_3N@C_{80}(I_h)$ (pink) in toluene.

Crystal Data for $CeSc_2N@C_{80}\cdot Ni^{II}(OEP)\cdot 2C_6H_6$: $C_{128}H_{56}CeN_5NiSc_2$, fw, 1952.51; black parallelepiped; crystal size, 0.10 × 0.07 × 0.04 mm^3; monoclinic; space group, *C*2/*c*; a = 25.3588(6) Å, b = 14.9668(3) Å, c = 39.4062(9) Å, β = 95.315(2)°, V = 14891.9(6) $Å^3$; λ(Mo Kα), 0.71073 Å; Z = 8, d_{calcd} = 1.742 Mg/m^3; μ(Mo Kα) = 1.096 mm^{-1}; $2\theta_{max}$ = 30.51°; T, 90(2) K; 120 547 refl. collected, 22 723 [R(int) = 0.0906] included in the refinement; 1242 parameters, no restraints, wR_2 = 0.117 for all data; conventional R_1 = 0.044 computed for 13 837 observed data with $I > 2\sigma(I)$.

Results and Discussion

Synthesis of the $Ce_xSc_{3-x}N@C_{80}$ (x = 0, 1) Family and Isolation of $CeSc_2N@C_{80}$. The vaporization of graphite rods packed with a mixture of Sc_2O_3, CeO_2, Fe_xN, and graphite powder was conducted in a Krätschmer−Huffman fullerene generator under a dynamic flow of helium and nitrogen gas, producing a black soot as shown in Scheme 1 and described in the Experimental Section. In contrast with the earlier reported $Er_xSc_{3-x}N@C_{80}$ (x = 0−3) family,[21] no significant peaks corresponding to $Ce_2ScN@C_{80}$ and $Ce_3N@C_{80}$ were observed in the NI-DCI mass spectrum. This is probably related to the greater lanthanide ion contraction for an erbium ion relative to a cerium ion (ionic radii: Er^{3+}, 103 pm vs Ce^{3+}, 115 pm).[37] Recently, we reported a new purification protocol to obtain pure TNT EMFs, $A_3N@C_{80}$ (A = lanthanide atom) directly from crude soots in a single, facile step based on the greater kinetic stablility of the TNT-EMFs relative to empty-cage fullerenes and classic EMFs, such as $A_x@C_{2y}$ (x = 1−3, y = 30−50).[38] Utilizing this method, the $CeSc_2N@C_{80}$ sample was isolated from the mixture. Final purification involved a two-stage, high-performance liquid chromatographic (HPLC) separation with the final HPLC trace and NI-DCI mass spectrum shown in Figure 1a.

Scheme 1

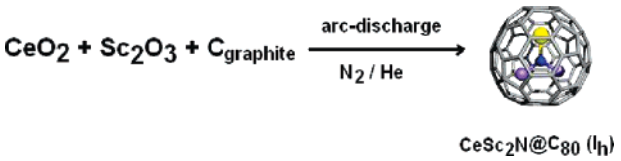

Electronic Structure of $CeSc_2N@C_{80}$. A. UV−visible Spectroscopy. A comparison of the UV−visible absorption spectra for $CeSc_2N@C_{80}$ and $Sc_3N@C_{80}$ metallofullerenes is illustrated in Figure 1c. Both molecules show similar absorption spectra. The $CeSc_2N@C_{80}$ UV−vis spectrum is similar to $Ce_2@C_{80}$,[16b] which also exhibits a monotonically decreasing absorption coefficient with increasing wavelength without well-defined sharp spectral features. Generally, the UV−vis spectrum of a metallofullerene depends on the cage structure (size and symmetry) as well as the charge on the cage. The similarities of these UV−vis spectra suggest that $Sc_3N@C_{80}$ and $CeSc_2N@C_{80}$ possess the same cluster charge transfer and I_h cage structure. These results, together with the ^{13}C NMR and XPS data described below, suggest that $CeSc_2N@C_{80}$ can be formally represented by $[CeSc_2N]^{+6}@[C_{80}]^{-6}$ which is similar to the formal charges found for $Sc_3N@C_{80}$[21] and $Ce_2@C_{80}$[16b].

B. XPS. The XPS binding energies for the Ce 3d core levels of $CeSc_2N@C_{80}$ are shown in Figure 2. The Ce region of the spectrum is quite similar to those of $Ce@C_{82}$ and $Ce_2@C_{80}$ with the two prominent features for the $3d_{3/2}$ and $3d_{5/2}$ levels. The binding energy of these two peaks (884.0 eV for $3d_{5/2}$ and 902.6 eV for $3d_{3/2}$) indicates the absence of Ce^{4+} in $CeSc_2N@C_{80}$, since Ce^{4+} has a characteristic 3d peak at a binding energy of approximately 914 eV arising from a transition from the initial state $3d^{10}4f^0$ to the final state $3d^94f^0$.[16b] Furthermore, the location and shape of the Ce (3d) peaks in the XPS spectrum of $CeSc_2N@C_{80}$ are quite similar to those of cerium trihalides,[39] suggesting that the Ce atom encaged in C_{80} is in the form of a Ce^{3+} ion. The carbon, scandium, and nitrogen binding energies are also consistent with those found for $Sc_3N@C_{80}$[21] and are illustrated in the Supporting Information.

NMR Studies of $CeSc_2N@C_{80}$. A. ^{13}C NMR. The ambient temperature ^{45}Sc and ^{13}C NMR spectra are shown in Figure 1b and related data are given in Table 1. The ^{13}C NMR spectrum of $CeSc_2N@C_{80}$ consists of two sharp signals in a 3/1 intensity ratio and is similar to those of $Sc_3N@C_{80}$ (I_h isomer),[21] $Lu_3N@C_{80}$ (I_h isomer),[28] and $Ce_2@C_{80}$.[40] It is surprising that

(37) Enghag, P. *Encyclopedia of the Elements: Technical Data, History, Processing, Applications*; Wiley-VCH: Weinheim, 2004; pp 386, 418.
(38) Ge, Z.; Duchamp, J. C.; Cai, T.; Gibson, H. W.; Dorn, H. C. *J. Am. Chem. Soc.* **2005**, *127*, 16292−16298.
(39) Suzuki, S.; Ishii, T.; Sagawa, T. *Physica Fennica* **1974**, *9*, 310−312.

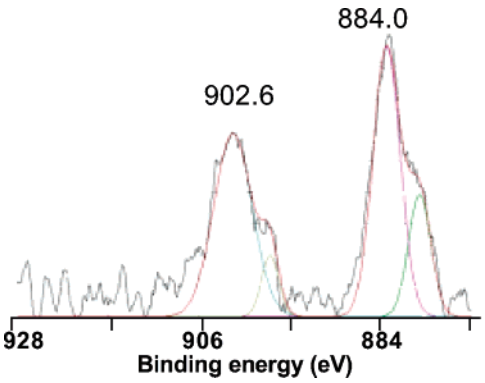

Figure 2. XPS spectrum of $CeSc_2N@C_{80}$ on a gold foil in the core level region of Ce (3d). The colored lines are fitting curves of the spectral peaks.

Table 1. Comparison of Chemical Shifts in ^{13}C NMR Spectra of Several Endohedral Metallofullerenes

metallofullerene	^{13}C NMR chemical shifts (ppm)	
$Sc_3N@C_{80}(I_h)$[21]	144.57	137.24
$Lu_3N@C_{80}(I_h)$[28]	144.0	137.4
$CeSc_2N@C_{80}$	142.85	135.90
$Ce_2@C_{80}$[40]	148.6	124.7

at ambient temperature the C_{80} cage carbon atoms are still isotropically motionally averaged yielding only two unique resonances even with the $CeSc_2N$ acentric top inside. These data and the ^{45}Sc NMR data below suggest a relatively small energy barrier for rotation of the $CeSc_2N$ cluster inside the carbon cage. The buried f electron spin of the $Ce^{3+}(4f^15d^0)$ ion produces only relatively minor effects on the ^{13}C NMR spectrum. For example, the only chemical shift difference between $CeSc_2N@C_{80}$ and $Sc_3N@C_{80}$ is a subtle upfield shift of approximately 1.5 ppm for both of the ^{13}C signals of $CeSc_2N@C_{80}$. In contrast, a somewhat larger ^{13}C NMR shift range was reported for $Ce_2@C_{80}$[40] which utilizes the same icosahedral cage $(C_{80})^{-6}$ but contains two encapsulated Ce^{3+} ions.

B. ^{45}Sc NMR. The dynamic behavior of the Sc atoms encapsulated in carbon cages is conveniently monitored by ^{45}Sc NMR. In a fashion similar to that of the data reported for the $Sc_2@C_{84}$ isomer (III)[41] and $Sc_3N@C_{80}$ (I_h),[21] the ^{45}Sc NMR spectrum for $CeSc_2N@C_{80}$ (Figure 1b) exhibits a single, symmetric peak at room temperature. Furthermore, when the temperature is raised from 313 K to 383 K, the ^{45}Sc NMR line width decreases from ~2700 Hz to ~1370 Hz (Figure 3). These results suggest that the internal motion provides the same average electronic environment for the two Sc atoms in the $CeSc_2N$ cluster. With the assumption that the correlation time can be expressed by $\zeta c = \zeta_0 \exp(E_a/kT)$,[41] where ζ_0 is a constant and E_a represents a rotation energy barrier, the line widths at different temperatures can be plotted to yield activation energy, $E_a = 79 \pm 6$ meV for the rotation energy barrier of $CeSc_2N@C_{80}$ in 1,2-dichlorobenzene. This energy barrier is the same as that of $Sc_3N@C_{80}$ I_h isomer (75 ± 8 meV in 1,2-dichlorobenzene; see Supporting Information) within the experimental error. However, it should be noted that this energy barrier is modulated by not only the internal motion of the endohedral cluster but also the overall rotational motion of the carbon cage.

The ^{45}Sc NMR chemical shift (δ) of $CeSc_2N@C_{80}$ exhibits a temperature-dependent Curie upfield chemical shift temperature

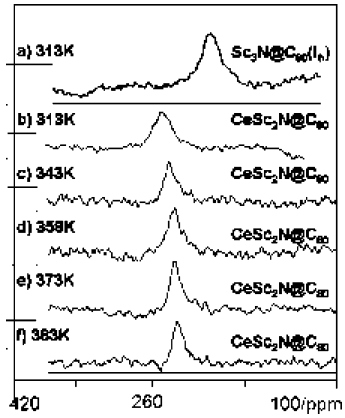

Figure 3. 97.2 MHz ^{45}Sc solution NMR spectra of $CeSc_2N@C_{80}$ in 1,2-dichlorobenzene (b−f) at various temperatures and $Sc_3N@C_{80}$ (I_h) in 1,2-dichlorobenzene (a) at 313 K.

that probably originates from the buried f electron spin remaining on the $Ce^{3+}(4f^15d^0)$ ion. As illustrated in Figure 3, a temperature increase from 313 K to 383 K yields an upfield shift in the resonance frequency of the ^{45}Sc signal from approximately 257.3 to 235.7 ppm (relative to external $ScCl_3$). As shown in the equation below, the chemical shifts of paramagnetic molecules in solution are generally composed of three contributions from diamagnetic (δ_{dia}), Fermi contact (δ_{fc}), and pseudocontact (δ_{pc}) shifts.[42]

$$\delta = \delta_{dia} + \delta_{fc} + \delta_{pc}$$

The paramagnetic term δ_{fc} is proportional to T^{-1} while δ_{pc} is proportional to T^{-2} (T = absolute temperature). Since the diamagnetic model molecule, $[CeSc_2N@C_{80}]^+$, was not available, the chemical shift of $Sc_3N@C_{80}$ was employed as the value of δ_{dia} in this case. The line-fitting plots of δ vs T^{-1} (see Supporting Information) showed the extrapolated value at $T^{-1} = 0$, 134.6 ppm, is quite different from the observed scandium chemical shift of 196.4 ppm for $Sc_3N@C_{80}$,[21] while the value extrapolated by the line-fitting plot with T^{-2} (see Supporting Information) at $T^{-2} = 0$, 189.9 ppm, is in reasonable agreement with the observed scandium shift of $Sc_3N@C_{80}$. Assuming our diamagnetic reference is appropriate, these results suggest that the pseudocontact (δ_{pc}) term dominates the chemical shift in a fashion similar to the situation reported for $Ce@C_{82}$.[43] A dominant Fermi contact interaction is also less likely, because it would only be possible via spin polarization transfer from Ce to the Sc nucleus through the Ce−N and N−Sc bonds.

Structure of $CeSc_2N@C_{80}$ as Determined by Single Crystal X-ray Diffraction. As previously shown,[21,22,35,44−47] cocrystallization of endohedral fullerenes with M^{II}(OEP) (M = Ni, Co; OEP is the dianion of octaethylporphyrin) is a useful method to obtain diffraction quality crystals, since most endohedral metallofullerenes themselves do not readily crystallize in an ordered fashion. Suitable crystals were obtained by diffusion of a benzene solution of Ni^{II}(OEP) into a solution of $CeSc_2N@C_{80}$ in benzene over a 2 week period. Black crystals with the composition $CeSc_2N@C_{80}\cdot Ni^{II}(OEP)\cdot 2C_6H_6$ were obtained and characterized by X-ray diffraction. Figure 4 shows a drawing

(40) Yamada, M. et al. *J. Am. Chem. Soc.* **2005**, *127*, 14570−14571.
(41) Miyake, Y.; Suzuki, S.; Kojima, Y.; Kikuchi, K.; Kobayashi, K.; Maniwa, Y.; Fischer, K. *J. Phys. Chem.* **1996**, *100*, 9579−9581.
(42) Bleaney, B. *J. Magn. Reson.* **1972**, *8*, 91−100
(43) Yamada, M.; Wakahara, T.; Lian, Y.; Tsuchiya, T.; Akasaka, T.; Waelchli, M.; Mizorogi, M.; Nagase, S.; Kadish, K. M. *J. Am. Chem. Soc.*, **2006**, *128*, 1400−1401

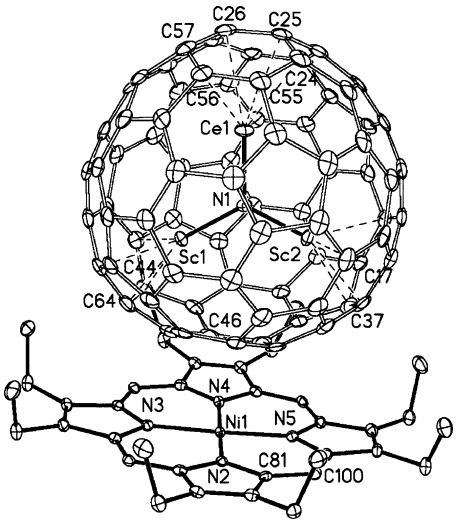

Figure 4. A perspective view of the relative orientations of $CeSc_2N@C_{80}$ and $Ni^{II}(OEP)$ within crystalline $CeSc_2N@C_{80}\cdot Ni^{II}(OEP)\cdot 2C_6H_6$. Thermal ellipsoids are shown at the 50% level.

of the endohedral and its relationship to the porphyrin. Both of these molecules reside in general positions and have no crystallographically imposed symmetry. In addition there is a molecule of benzene in a general position and two others at half occupancy, each located on a two-fold axis.

Endohedrals that are cocrystallized with metalloporphyrins can show some degree of disorder in either the cage orientation, in the location of the metal ions inside the cage, or both.[21,22,28b,35,46,47] However, in $CeSc_2N@C_{80}\cdot Ni^{II}(OEP)\cdot 2C_6H_6$, the fullerene cage and the $CeSc_2N$ unit are both *fully ordered*. The C_{80} unit has the I_h isomeric structure, which is generally the more abundant of the two cage isomers (I_h and D_{5h}) so far observed in C_{80}-containing endohedrals. Inside the cage, the two scandium ions are situated in close proximity to the metalloporphyrin, while the cerium ion is located on the far side of the cage. The Sc2−N−Sc1angle is 116.87(12)°, and the Sc2−N−Ce and Sc1−N−Ce angles are 121.67(11)° and 121.45(11)°, respectively. The $CeSc_2N$ unit is planar, since the sum of these three angles about the central nitrogen is 359.99°. Previous studies have shown that the trimetallic nitride cluster is planar in the cases of $Sc_3N@C_{80}$,[21] $ErSc_2N@C_{80}$,[35] $Sc_3N@C_{78}$,[47] $Sc_3N@C_{68}$,[46] and $Lu_3N@C_{80}$,[28b] although the cage sizes and geometries vary significantly in these TNT endohedral fullerenes. In contrast, due to the large size of Gd(III), the Gd_3N unit in $Gd_3N@C_{80}$,[22] is pyramidal with the nitrogen atom displaced by 0.522(8) Å from the plane of the three gadolinium ions.

As might be expected on the basis of ionic radii, the Ce−N distance, 2.184(2) Å, in $CeSc_2N@C_{80}$ is considerably longer than the Sc1−N and Sc2−N distances, 1.942(2) and 1.933(2) Å, respectively. For comparison the Sc−N distances are longer in related endohedrals: 1.9931(14), 2.0323(16), and 2.0526-(14) Å in the I_h isomer of $Sc_3N@C_{80}$;[21] 1.988(7), 1.983(15), and 2.125(5) in $Sc_3N@C_{78}$;[47] and 1.961(4), 1.974(4), and 2.022-(3) in $Sc_3N@C_{68}$.[46] Note that the cage size is reduced in the latter two endohedrals and yet the Sc−N distances are still longer than those in $CeSc_2N@C_{80}$ where the large cerium ion acts to compress the two Sc−N bonds. Also notice that in $ErSc_2N@C_{80}$ the Sc−N distance, 1.968(6) Å, is longer than the Sc−N distances in $CeSc_2N@C_{80}$, while the Er−N distance, 2.089(9) Å, is shorter than the Ce−N distance. The large size of the cerium ion also pushes N1 0.36 Å away from the center of the C_{80} cage and toward the two scandium ions.

Figure 5 shows the locations of the metal ions relative to the cage. The figure consists of projections of the metal ions onto the least squares planes of the carbon atoms as viewed from the inside of the cage. The cerium ion is positioned above the center of a hexagon. In contrast the scandium ions are located near 6:5 ring junctions with a displacement toward the hexagon. The metal ion placement differs from that seen in $ErSc_2N@C_{80}$ where all the metal ions lie over carbon atoms at the intersection of two hexagons and one pentagon.[35]

Consideration of the pyramidalization of the carbon atoms in the C_{80} cage as measured by θ_p[44] (θ_p for graphite = 0°; θ_p for C_{60} = 11.6°) reveals that the adjacent metal ions inside and outside the cage exert a measurable effect on the cage structure of $CeSc_2N@C_{80}$. Figure 6 shows a plot of θ_p for all of the cage carbon atoms in $CeSc_2N@C_{80}\cdot Ni^{II}(OEP)\cdot 2C_6H_6$. In the I_h C_{80} cage, there are two types of carbon atoms: 60 (show as squares in Figure 6) are part of pentagons, while 20 others (shown as circles) do not reside in pentagons but are located at the confluence of three hexagons. The carbon atoms that are part of pentagons have an average θ_p of 9.92(6)°, while those at the confluence of three hexagons have an average θ_p of 8.82(2)°. In calculating these averages we have omitted carbon atoms near the metal centers since these metal ions perturb the cage geometry. Thus, the four carbon atoms (C17, C37, C44, and C64) nearest to scandium atoms with Sc−C distances in the range 2.34−2.39 Å have the highest pyramidalization and appear as deep pink squares in Figure 6. The six carbon atoms that surround the cerium ion also have elevated values: these are shown in blue. Also the four carbon atoms (deep pink circles) that are 2.34−2.39 Å from one of the scandium ions exhibit elevated values of θ_p. Thus, the pattern clearly emerges that the carbon atoms near internal metal ions show enhanced pyramidalization. In contrast, the carbon atom (C46) nearest the external nickel ion in the porphyrin shows a reduced θ_p value of 8.3 when compared to other carbon atoms like it that are part of pentagons. This observation is consistent with the situation seen in another well-ordered endohedral structure, that of the D_{5h} isomer of $Sc_3N@C_{80}\cdot Ni(OEP)\cdot 2$benzene, where again the carbon atoms nearest the nickel ion are slightly flatted.[33]

Conclusions

In summary, $CeSc_2N@C_{80}$, a TNT endohedral metallofullerene with a nitrogen atom offset from its center and buried f electron spin, has been synthesized and isolated in high purity. The purified $CeSc_2N@C_{80}$ has been characterized by mass spectrometry, ^{13}C and ^{45}Sc NMR spectroscopy, UV−vis spectroscopy, XPS spectroscopy, and a single-crystal X-ray diffraction study of the cocrystallized solid, $CeSc_2N@C_{80}\cdot Ni(OEP)\cdot 2C_6H_6$. The ^{13}C NMR spectrum of $CeSc_2N@C_{80}$ exhibits two lines with a 3:1 intensity ratio, indicating that the C_{80} cage has I_h symmetry. The similarities of UV−vis spectra between

(44) Haddon, R. C.; Raghavachari, K. In *Buckminsterfullerenes*; Billups, W. E.; Ciufolini, M. A., Eds.; VCH: New York, 1993; Chapter 7.
(45) Reich, A.; Panthofer, M.; Modrow, H.; Wedig, U.; Jansen, M. *J. Am. Chem. Soc.* **2004**, *126*, 14428−14434.
(46) Olmstead, M. M.; Lee, H. M.; Duchamp, J. C.; Stevenson, S.; Marciu, D.; Dorn, H. C.; Balch, A. L. *Angew. Chem., Int. Ed.* **2003**, *42*, 900−902.
(47) Olmstead, M. M.; de Bettencourt-Dias, A.; Duchamp, J. C.; Stevenson, S.; Marciu, D.; Dorn, H. C.; Balch, A. L. *Angew. Chem., Int. Ed.* **2001**, *40*, 1223−1225.

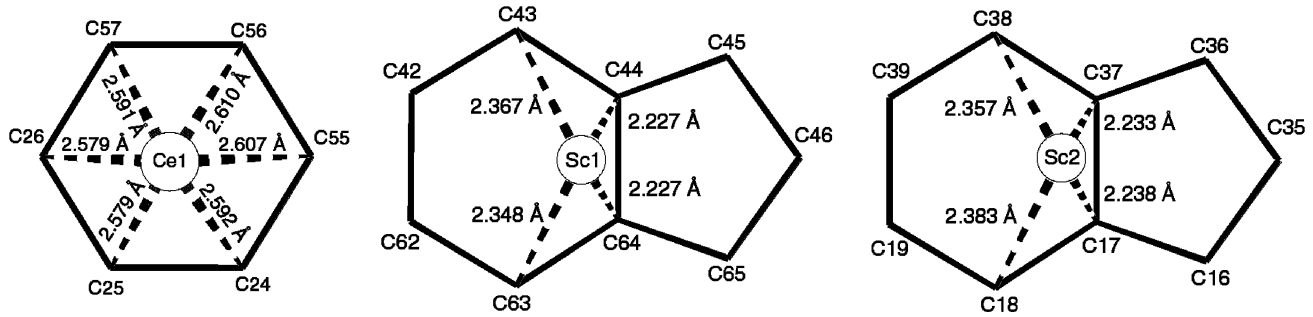

Figure 5. Drawings that show the positions of the metal ions with respect to the adjacent walls of the C_{80} cage in $CeSc_2N@C_{80}{\cdot}Ni^{II}(OEP){\cdot}2C_6H_6$. The metal ions are projected onto the least-squares planes of the sets of carbon atoms shown as seen from the inside of the cage.

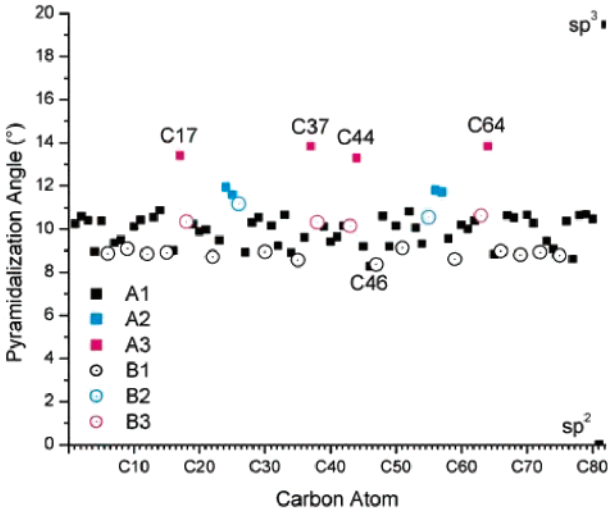

Figure 6. Pyramidalization angles, θ_p, for the carbon atoms in $CeSc_2N@C_{80}$. The 60 carbon atoms that are part of pentagons are shown as squares, while the 20 others that do not reside in pentagons are shown as circles. Carbon atoms nearest internal metal atoms are colored (deep pink for the atoms near a scandium ion, blue for atoms near a cerium atom), and the remaining carbon atoms are represented by black symbols. A1 and B1, carbon atoms with no close contact with metal atoms inside the cage; A2, carbon atoms in pentagons near Ce; A3, carbon atoms in pentagons near Sc; B2, carbon atoms not in pentagons near Ce; B3, carbon atoms not in pentagons near Sc.

$CeSc_2N@C_{80}$, $Sc_3N@C_{80}$, and $Ce_2@C_{80}$ suggest that the $CeSc_2N@C_{80}$ can be formally represented by $[Ce^{III}Sc^{III}_2N^{-III}]^{+6}@[C_{80}]^{-6}$. The XPS pattern of the Ce 3d core level in $CeSc_2N@C_{80}$ indicates a +3 valence state of cerium. The internal motion of the trimetallic nitride cluster was demonstrated by ^{45}Sc NMR. The rotation activation barrier is approximately 79 meV, which is nearly the same as that of $Sc_3N@C_{80}$ (75 meV) within the experimental error range. Also, the temperature-dependent ^{45}Sc NMR study reveals the paramagnetic nature of $CeSc_2N@C_{80}$. The crystallographic characterization indicates the structure of $CeSc_2N@C_{80}$ consists of a planar $CeSc_2N$ unit surrounded by an icosahedral C_{80} cage. The cerium ion within the cage is positioned below the center of a hexagon, while the scandium ions are located near 6:5 ring junctions with displacements toward the hexagons. Due to the large size of the Ce ion, the N atom is pushed 0.36 Å away from the central position toward the two scandium ions, which makes the compressed Sc−N bond lengths even shorter than those in $Sc_3N@C_{68}$ (1.942(2) and 1.933(2) in $CeSc_2N@C_{80}$ vs 1.961(4), 1.974(4), and 2.022-(3) in $Sc_3N@C_{68}$).

Acknowledgment. The authors thank Anne Campell for her technical assistance in acquiring the NI-DCI mass spectrum and the National Science Foundation (Grants CHE-0443850 and DMR-0507083 to H.C.D. and CHE-0413857 to A.L.B.) for support. Also, we acknowledge support from National Institute of Health [1R01-CA119371-01 (H.C.D.)].

Supporting Information Available: Complete refs 21 and 40, HPLC traces of the extracts before and after chemical separation, a portion of NI-DCI mass spectrum of the extracts, XPS spectrum of $CeSc_2N@C_{80}$ in the core level regions of Sc, N, and C, 121.5 MHz ^{45}Sc NMR spectra of $Sc_3N@C_{80}(I_h)$ in 1,2-dichlorobenzene at various temperatures, line-fitting plots for ^{45}Sc NMR (chemical shift vs T^{-1} and chemical shift vs T^{-2}). X-ray crystallographic data files in CIF format for $CeSc_2N@C_{80}{\cdot}Ni^{II}(OEP){\cdot}2C_6H_6$. This material is available free of charge via the Internet at http://pubs.acs.org.

JA061434I